

Theory of spin-orbit coupling at LaAlO₃/SrTiO₃ interfaces and SrTiO₃ surfaces

Zhicheng Zhong, Anna Tóth, and Karsten Held

Institute of Solid State Physics, Vienna University of Technology, A-1040 Vienna, Austria

(Received 4 July 2012; published 5 April 2013)

The theoretical understanding of the spin-orbit coupling (SOC) effects at LaAlO₃/SrTiO₃ interfaces and SrTiO₃ surfaces is still in its infancy. We perform first-principles density-functional-theory calculations and derive from these a simple tight-binding Hamiltonian, through a Wannier function projection and group theoretical analysis. We find striking differences to the standard Rashba theory for spin-orbit coupling in semiconductor heterostructures due to multiorbital effects: By far the biggest SOC effect is at the crossing point of the xy and yz (or zx) orbitals, and around the Γ point a Rashba spin splitting with a cubic dependence on the wave vector \vec{k} is possible.

DOI: [10.1103/PhysRevB.87.161102](https://doi.org/10.1103/PhysRevB.87.161102)

PACS number(s): 73.20.-r, 73.21.-b, 79.60.Jv

I. INTRODUCTION

Very recently, Caviglia *et al.*¹ and Ben Shalom *et al.*² studied the magnetotransport properties of the high mobility two-dimensional electron gas (2DEG) at the interface between two insulating perovskite oxides, LaAlO₃ (LAO) and SrTiO₃ (STO).³ They found strong spin-orbit coupling (SOC) effects, whose magnitudes can even be tuned by gate voltages. This strong SOC has been the basis for many subsequent theoretical and experimental studies.⁴⁻⁹ Despite its increasing importance, a clear physical picture of the SOC effects in LAO/STO interfaces is still missing.

SOC generally originates from the relativistic correction $(\hbar/2m_e^2c^2)(\nabla V \times \vec{p}) \cdot \vec{s}$ to the Schrödinger equation, with m_e being the free electron mass and V the potential in which the electrons move with momentum \vec{p} and spin \vec{s} . If $V(r)$ has spherical symmetry like in atoms or approximately in solids, the form can be reduced to $\xi(r)\vec{l} \cdot \vec{s}$, where $\xi(r)$ denotes the strength of the atomic SOC, and \vec{l} and \vec{s} are the orbital and spin angular momenta of the electron. Thus SOC lifts orbital and spin degeneracies. For a cubic perovskite such as STO, the six initially degenerate t_{2g} orbitals at the Γ point are indeed split by SOC,¹⁰⁻¹³ but Kramers degeneracy (time-reversal symmetry) is preserved. Because bulk STO has both crystal inversion symmetry $\varepsilon(\vec{k}, \uparrow) = \varepsilon(-\vec{k}, \uparrow)$ and time-reversal symmetry $\varepsilon(\vec{k}, \uparrow) = \varepsilon(-\vec{k}, \downarrow)$, the energy ε at wave vector \vec{k} is still spin degenerate.

This changes for a LAO/STO interface since the inversion symmetry is broken so that the SOC lifts the spin degeneracy of the 2DEG. This two-dimensional SOC effect is known as Rashba spin splitting, which has been widely studied in semiconductor heterostructures^{14,15} and metal surfaces.¹⁶ Assuming a nearly free 2DEG with effective mass m , its two spin components will be split by $\Delta_R = 2\alpha_R k$, where the Rashba coefficient $\alpha_R = (\hbar/4m^2c^2)dV(z)/dz$ depends on the potential gradient in the z direction (perpendicular to the interface). Naively, since an electric field gives rise to an electrostatic potential gradient, Δ_R seems to be simply proportional to the gate voltage. However, a typical electric field in experiments is ~ 100 V/mm yielding, according to the formula above, $\Delta_R \sim 10^{-8}$ meV,¹⁴ which is much smaller than the measured values of the order of meV.^{1,2} This is because the assumption of nearly free 2DEG, which ignores the

region of ion cores and the asymmetric feature of the interface wave function, is too simple. In reality, the expression for Δ_R is much more complicated¹⁷⁻²¹ and usually treated as a fitting parameter in semiconductor heterostructures and metal surfaces.

The aim of this Rapid Communication is the theoretical description of SOC in oxide heterostructures and surfaces. From density-functional-theory (DFT) calculations we derive a tight-binding (TB) Hamiltonian for the low energy t_{2g} orbitals and their spin splitting. In particular, we show that besides the standard k -linear Rashba spin splitting, there can be a k -cubic spin splitting around the Γ point due to multiorbital effects. A much larger spin splitting occurs at the crossing point of the xy and yz (or zx) orbitals.

II. METHOD

Besides bulk STO, we calculate (i) LAO/STO (1.5/6.5 layers),^{22,23} which is symmetric with two n -type interfaces; (ii) LAO/STO (4/4) and (1/1), which is asymmetric with n - and p -type interfaces;²⁴ (iii) vacuum/LAO/STO (3/1/4), which has a single n -type interface;^{25,26} and (iv) vacuum/STO (3/7.5) with a SrO terminated surface. We fix the in-plane lattice constant of the supercells to the calculated equilibrium value of STO, and optimize the internal coordinates. The DFT calculations have been done using the WIEN2K code with the generalized gradient approximation.^{27,28} The SOC is included as a perturbation using the scalar-relativistic eigenfunctions of the valence states. Through a projection onto maximally localized Wannier orbitals,²⁹⁻³¹ we construct a realistic TB model, and in particular, we develop a way to describe the interface asymmetry.

III. DFT RESULTS FOR STO

Bulk SrTiO₃ is a band insulator with an energy gap between occupied O_{2p} bands and unoccupied $Ti_{3d} t_{2g}$ (yz, zx, xy) bands. The t_{2g} band structure calculated by DFT is shown in Fig. 1(a). In the absence of SOC, the three t_{2g} orbitals are degenerate at $\Gamma(0,0,0)$ due to an octahedral O_h crystal field around the Ti atoms in a perfect perovskite structure. Around Γ the bands can be fit by a parabolic function of the form $\hbar^2 k^2/2m^*$ where the effective mass m^* depends on the orbital and the direction.

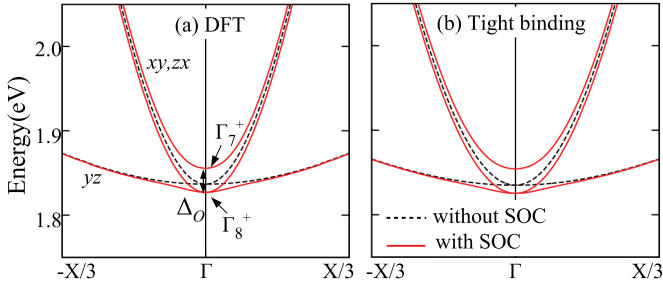


FIG. 1. (Color online) Band structure of t_{2g} orbitals in bulk SrTiO₃ calculated by (a) DFT and by (b) a TB model derived in this Rapid Communication. In the absence of spin-orbit coupling, yz , zx , and xy are degenerate at the Γ point. SOC splits the sixfold-degenerate orbitals into Γ_7^+ and Γ_8^+ states separated by $\Delta_0 = 29$ meV.

Along the Γ - $X(\pi,0,0)$ direction (here in units of $1/a$ with $a = 3.92$ Å being the calculated lattice constant of STO), the yz band has a small energy dispersion corresponding to a heavy mass of $6.8m_e$. In contrast, the zx and xy orbitals have the same, large energy dispersion and a light effective mass of $0.41m_e$. Including the SOC, the sixfold-degenerate orbitals are split into a doubly and a fourfold-degenerate level with an orbital splitting of $\Delta_0 = 29$ meV (Ref. 13) (see Fig. 1). The energy dispersion of the resulting orbitals is now considerably different from the initial orbitals. Consequently, the corresponding effective masses around Γ are changed to 1.39, 0.41, and $0.53m_e$, respectively.

IV. TB HAMILTONIAN FOR STO

To understand the DFT results, we use a Wannier projection to obtain the local energy and hopping terms of the t_{2g} orbitals. Without SOC, the constructed three-band TB Hamiltonian of bulk STO H_0^b can be expressed in the t_{2g} basis in a matrix form: One of the diagonal terms is $\langle xy|H_0^b|xy\rangle = \varepsilon_0^{xy} - 2t_1 \cos k_x - 2t_1 \cos k_y - 2t_2 \cos k_z - 4t_3 \cos k_x \cos k_y$; The other two follow by exchanging the x, y, z indices. The local energy term is $\varepsilon_0 = 3.31$ eV for all three orbitals. The large hopping $t_1 = 0.277$ eV stems from the large xy intraorbital hopping integral along the x and y directions; it is due to two lobes of xy orbitals at the nearest-neighbor sites pointing to each other along the two directions. In contrast, $t_2 = 0.031$ eV and $t_3 = 0.076$ eV indicate a much smaller hopping integral along the z and $(1,1,0)$ directions, respectively. We find all orbital-off-diagonal (interorbital hopping) terms to be negligible. The TB energy dispersion for the three orbitals is plotted in Fig. 1(b), showing good agreement with the DFT results.

We include SOC at the atomic level as $H_\xi = \xi \vec{l} \cdot \vec{s}$, where ξ is the atomic SOC strength and depends on atomic numbers. Under the O_h crystal field, the six spinful t_{2g} orbitals break into a doublet $|\Gamma_7^+, \pm \frac{1}{2}\rangle \equiv \frac{1}{\sqrt{3}}(-i yz|\downarrow, \uparrow) \pm zx|\downarrow, \uparrow) \mp ixy|\uparrow, \downarrow)$, and a quartet $|\Gamma_8^+, \pm \frac{1}{2}\rangle \equiv \frac{1}{\sqrt{2}}(\mp i yz - zx)|\downarrow, \uparrow)$, $|\Gamma_8^+, \pm \frac{3}{2}\rangle \equiv \frac{1}{\sqrt{6}}(\pm i yz|\uparrow, \downarrow) + zx|\uparrow, \downarrow) + 2ixy|\downarrow, \uparrow)$.³²

H_ξ lifts their degeneracy at the Γ point and is diagonal in the Γ_7^+, Γ_8^+ basis with eigenvalues of ξ and $-\xi/2$, respectively. We set $\xi = 2\Delta_0/3 = 19.3$ meV, which leads to the same orbital splitting as the DFT results. In the original t_{2g} basis

$(yz|\uparrow), yz|\downarrow), zx|\uparrow), zx|\downarrow), xy|\uparrow), xy|\downarrow)$, H_ξ has off-diagonal terms and reads

$$\frac{\xi}{2} \begin{pmatrix} 0 & 0 & i & 0 & 0 & -1 \\ 0 & 0 & 0 & -i & 1 & 0 \\ -i & 0 & 0 & 0 & 0 & i \\ 0 & i & 0 & 0 & i & 0 \\ 0 & 1 & 0 & -i & 0 & 0 \\ -1 & 0 & -i & 0 & 0 & 0 \end{pmatrix}.$$

$H_0^b + H_\xi$ is the TB Hamiltonian of bulk STO including SOC. Its band structure is shown as a solid line in Fig. 1(b) and agrees well with the DFT results. This model allows for a deeper understanding of the SOC effects: The SOC eigenstates are admixtures of the yz , zx , and xy orbitals, which explains the significant changes of the effective masses.

V. DFT RESULTS FOR INTERFACES

The band structure of LAO/STO (1.5/6.5) calculated by DFT is shown in Fig. 2(a). Without SOC, similar to bulk STO, all bands exhibit a paraboliclike behavior. In the x direction, the yz band is the flattest (heaviest); at Γ , it is degenerate with the zx . Due to the interface, the xy band is $\Delta_I = 250$ meV lower in energy at Γ than the degenerate yz and zx bands. The splitting Δ_I is the most notable feature of the heterostructure.^{22,23,26} It is not mainly a crystal field effect, but originates from the vanishing of the hopping from the interface Ti yz to LAO along the z direction.³¹ Consistently, a similar behavior is expected in a SrO terminated STO surface, and indeed we obtain it

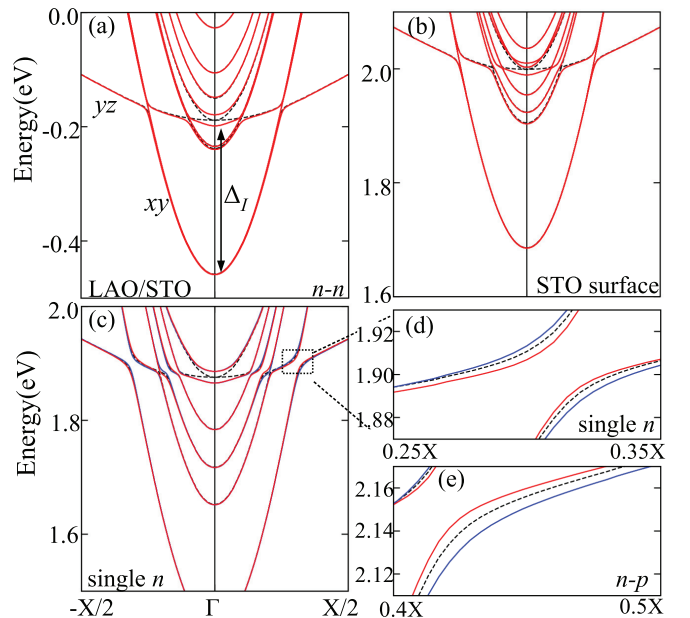


FIG. 2. (Color online) DFT calculated band structure of (a) LAO/STO with two symmetric n -type interfaces; (b) SrO terminated STO surface; and (c) vacuum/LAO/STO with a single n -type interface. The region with biggest spin splitting around the xy - yz crossing point is magnified in (d) and for a LAO/STO (4/4) with asymmetric n - p interfaces in (e). Δ_I denotes the interface induced orbital splitting energy; the black dashed line is without SOC; the red and blue solid lines are the two opposite spin channels with SOC.

with $\Delta_I = 320$ meV [see Fig. 2(b)]. Our calculated splittings are qualitatively consistent with the ARPES measurements of STO surfaces.^{33,34}

Including SOC does not influence the xy band very much. It splits the degenerate yz and zx orbitals with $\Delta_O = 19$ meV at Γ [see Fig. 2(a)]. The *ab initio* calculated Δ_O is qualitatively consistent with experiment, albeit smaller than its experimental value³³ $\Delta_O = 60$ meV. Around Γ , the effective masses for xy and the resulting two states are 0.48, 1.14, and $0.72m_e$, respectively. For the asymmetric case Fig. 2(c) the SOC also results in a spin splitting which is most noticeable at the xy - yz crossing region where it is up to 18 meV [see Figs. 2(d) and 2(e)]. This spin splitting is a multiorbital effect, very different from the standard Rashba spin splitting of single orbital. For a better understanding, we now construct a TB Hamiltonian.

VI. SPIN SPLITTING AT THE INTERFACE LAYER

Without SOC, a model Hamiltonian H_0^i can describe the interface hopping and the induced splitting Δ_I . In contrast to H_0^b , the hopping terms of H_0^i in direction z essentially vanish. The diagonal term for xy is hence $\varepsilon^{xy} - 2t_1 \cos k_x - 2t_1 \cos k_y - t_2 - 4t_3 \cos k_x \cos k_y$, while that for the yz (and zx) orbital is $\varepsilon^{yz} - 2t_2 \cos k_x - 2t_1 \cos k_y - t_1 - 2t_3 \cos k_y$. The local energy terms $\varepsilon^{xy/yz}$ will be influenced by the interface crystal field, electron filling, and confinement.^{23,26,31} For simplicity, we approximate these by the bulk value ε_0 . Thus, $\Delta_I = t_1 - t_2 + 2t_3 = 0.4$ eV, which is comparable to the DFT results. At the interface the O_h symmetry breaks down to C_{4v} , and we can use the same atomic SOC H_ξ matrix as before, since under C_{4v} the Γ_7^+ doublet does not break, whereas the Γ_8^+ quartet breaks into $\Gamma_6^+ \oplus \Gamma_7^+$, with the same set of basis functions as given previously. The $H_0^i + H_\xi$ Hamiltonian gives an atomic SOC induced orbital splitting about $\Delta_O = \sqrt{5}\xi/2$ at Γ similar to Figs. 2(a)–2(c). However $H_0^i + H_\xi$ does not contain any terms breaking the interface inversion symmetry, and hence it does not include the Rashba spin splitting.

To this end, we introduce a term H_γ to describe the broken inversion symmetry at the interface, a key component for Rashba spin splitting. The essential physics of this term was analyzed by Lashell *et al.*¹⁶ and then introduced by Petersen *et al.*³⁶ to construct a TB model for the Rashba effects of s - p orbitals in metal surfaces. To our knowledge, there and in other publications, H_γ was always treated as a parameter and hence its utility and importance are strongly limited. In this study, we project the DFT results above onto maximally localized Wannier orbitals³¹ and then directly extract the spin independent hopping term H_γ ,

$$\gamma \begin{pmatrix} 0 & 0 & 2i \sin k_x \\ 0 & 0 & 2i \sin k_y \\ -2i \sin k_x & -2i \sin k_y & 0 \end{pmatrix}$$

describing interorbital hopping terms due to the interface asymmetry. The key hopping term is $\gamma = \langle xy|H|yz(R) \rangle$, where R is the nearest neighbor in the x direction. As shown in the schematic Fig. 3(a), γ is an antisymmetric hopping between xy and yz orbitals along the x direction. Its origin

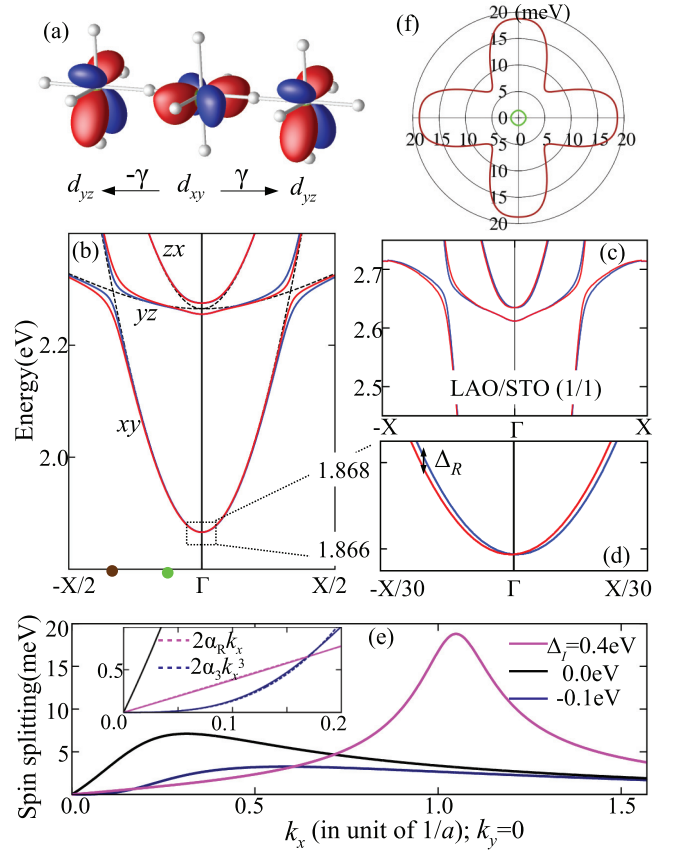


FIG. 3. (Color online) (a) Schematic figure of the orbital deformation at the interface resulting in an antisymmetric hopping term γ . Band structures calculated by (b) TB Hamiltonian $H_0^i + H_\xi + H_\gamma$ [the dashed line shows H_0^i only (Ref. 35)], and by (c) DFT for comparison. (d) The standard Rashba spin splitting Δ_R can be observed after zooming in the band structure of panel (b); red and blue indicate opposite spin. (e) Spin splitting in the lowest band of the TB Hamiltonian for different Δ_I . The inset shows a k_x -linear (-cubic) spin splitting for positive (negative) Δ_I . (f) Angular dependence of the spin splitting at the standard Rashba region (green) and the xy - yz/zx crossing region (brown) at the \vec{k} points displayed in (b).

is the interface asymmetry deforming the orbital lobes of the interface layer. We find $\gamma \sim 20$ meV at the n -type interface for all geometries, and hence take this value in the model. Let us note γ drops quickly in the second and further layers towards its bulk value $\gamma = 0$.

The combined model Hamiltonian $H_0^i + H_\xi + H_\gamma$, including Rashba effects, is expressed in the t_{2g} basis by a 6×6 matrix, where H_0^i describes the interface hopping and splitting Δ_I , H_ξ includes the atomic SOC and accounts for the orbital splitting of Δ_O , and H_γ describes the interface asymmetry. The first effect is a standard Rashba type of spin splitting in the single xy band. It splits a single parabola around the minimum at Γ into two parabolas with opposite spin [see Fig. 3(d)]. By downfolding the matrix onto an effective Hamiltonian for the xy band, we obtain an analytical expression for the spin splitting $\Delta_R = 2\alpha_R k_x$ with $\alpha_R = 2a\xi\gamma/\Delta_I = 0.76 \times 10^{-2}$ eV \AA for $\Delta_I = 0.4$ eV, $\xi = 19.3$ meV, and $\gamma = 20$ meV. Note that Δ_I depends strongly on the details of the interface and

hence α_R can be up to eight times larger at $\Delta_I = 0$ where the formula above does not hold anymore [see Fig. 3(e)]. This well agrees with the experimental magnitude of the Rashba spin splitting $\alpha_R = 1-5 \times 10^{-2} \text{ eV \AA}^1$.

If we turn Δ_I negative, which is possible by interface engineering,³¹ the lowest band is a mixture of yz and zx . In this situation there is no standard k -linear Rashba effect anymore but we obtain a spin splitting $2\alpha_3 k_x^3$ with $\alpha_3 = 4 \text{ eV \AA}^3$ [see Fig. 3(e)]. Hence, the TB model also explains qualitatively and quantitatively the unusual k -cubic spin splitting reported in Ref. 37 in a single framework, reconciling the puzzling discrepancy between experiments of Refs. 37 and 1.

An even much bigger spin splitting 18 meV occurs, however, at the xy - yz crossing point [see Figs. 3(b), 3(c), and 3(e) and Figs. 2(c)–2(e)]. Unlike the isotropic splitting Δ_R around Γ , this spin splitting is not only much larger but also anisotropic [see Fig. 3(f)]. This multiband effect is a particularity of transition-metal oxides and not occurring in semiconductors or metal surfaces. Experimentally, a similar anisotropy has been observed in LAO/STO heterostructures with a particular strong SOC effect.^{38,39}

An important aspect of our study is also that the external electric field^{1,2} does not significantly tune the SOC directly. As mentioned in the Introduction, its direct contribution is too small. Even without it, we obtain the correct magnitude of the spin splitting. Nonetheless, the spin splitting depends on the electric field.^{1,2} The explanation for this is an indirect effect: The electric field tunes the carrier densities,^{40–44} band filling,^{23,26,45,46} and the effective γ . The multiorbital complexity might account for the discrepancy of the two reported spin energies tuned by gate voltages.^{1,2}

VII. CONCLUSION

We performed first-principle calculations and developed a realistic three-band (xy , yz , and zx) model for SOC effects at LAO/STO interfaces and STO surfaces. The key ingredients to the spin splitting are the atomic SOC and the interface asymmetry, which enters via asymmetric t_{2g} orbital lobes. The xy orbital around Γ exhibits the standard Rashba spin splitting $2\alpha_R k$ with $\alpha_R = 2a\xi\gamma/\Delta_I \sim 10^{-2} \text{ eV \AA}$; in contrast, for negative Δ_I there is instead a k -cubic dependence spin splitting in the lowest band around Γ . As Δ_I depends on the particular surface or interface, this solves the experimental controversy regarding linear or cubic Rashba splitting. Even more importantly, we find an unusually large spin splitting 18 meV at the crossing point of xy and yz/zx orbitals. Our results indicate that LAO/STO has peculiar SOC properties arising from the multiorbital character which are absent in the standard single-band description as for the nearly free 2DEG in semiconductor heterostructures.

Note added. The same tight-binding model and physical results have also been presented in Ref. 47.

ACKNOWLEDGMENTS

We are grateful to G. Sangiovanni, P. Wissgott, R. Arita, V. I. Anisimov, and P. J. Kelly for useful discussions. Z.Z. and K.H. acknowledge funding from the SFB ViCoM (Austrian Science Fund project ID F4103-N13), A.T. from the European Research Council under Grant No. FP7-ERC-227378 and from the EU-Indian network MONAMI and the Austrian Ministry for Science and Research (BM.W_F). Calculations have been done on the Vienna Scientific Cluster (VSC).

¹A. D. Caviglia, M. Gabay, S. Gariglio, N. Reyren, C. Cancellieri, and J.-M. Triscone, *Phys. Rev. Lett.* **104**, 126803 (2010).

²M. Ben Shalom, M. Sachs, D. Rakhmilevitch, A. Palevski, and Y. Dagan, *Phys. Rev. Lett.* **104**, 126802 (2010).

³A. Ohtomo and H. Y. Hwang, *Nature (London)* **427**, 423 (2004).

⁴K. Michaeli, A. C. Potter, and P. A. Lee, *Phys. Rev. Lett.* **108**, 117003 (2012).

⁵N. Reyren, M. Bibes, E. Lesne, J.-M. George, C. Deranlot, S. Collin, A. Barthélemy, and H. Jaffrès, *Phys. Rev. Lett.* **108**, 186802 (2012).

⁶L. Fidkowski, H.-C. Jiang, R. M. Lutchyn, and C. Nayak, *Phys. Rev. B* **87**, 014436 (2013).

⁷S. Caprara, F. Peronaci, and M. Grilli, *Phys. Rev. Lett.* **109**, 196401 (2012).

⁸M. H. Fischer, S. Raghu, and E.-A. Kim, *New J. Phys.* **15**, 023022 (2013).

⁹A. Fête, S. Gariglio, A. D. Caviglia, J.-M. Triscone, and M. Gabay, *Phys. Rev. B* **86**, 201105(R) (2012).

¹⁰L. F. Mattheiss, *Phys. Rev. B* **6**, 4718 (1972).

¹¹A. Janotti, D. Steiauf, and C. G. Van de Walle, *Phys. Rev. B* **84**, 201304 (2011).

¹²R. Bistritzer, G. Khalsa, and A. H. MacDonald, *Phys. Rev. B* **83**, 115114 (2011).

¹³D. van der Marel, J. L. M. van Mechelen, and I. I. Mazin, *Phys. Rev. B* **84**, 205111 (2011).

¹⁴R. Winkler, *Spin Orbit Coupling Effects in Two-Dimensional Electron and Hole Systems* (Springer, New York, 2003).

¹⁵J. Nitta, T. Akazaki, H. Takayanagi, and T. Enoki, *Phys. Rev. Lett.* **78**, 1335 (1997).

¹⁶S. LaShell, B. A. McDougall, and E. Jensen, *Phys. Rev. Lett.* **77**, 3419 (1996).

¹⁷G. Lommer, F. Malcher, and U. Rossler, *Phys. Rev. Lett.* **60**, 728 (1988).

¹⁸T. Schapers, G. Engels, J. Lange, T. Klocke, M. Hollfelder, and H. Luth, *J. Appl. Phys.* **83**, 4324 (1998).

¹⁹G. Nicolay, F. Reinert, S. Hüfner, and P. Blaha, *Phys. Rev. B* **65**, 033407 (2001).

²⁰G. Bihlmayer, Y. Koroteev, P. Echenique, E. Chulkov, and S. Blügel, *Surf. Sci.* **600**, 3888 (2006).

²¹M. Nagano, A. Kodama, T. Shishidou, and T. Oguchi, *J. Phys.: Condens. Matter* **21**, 064239 (2009).

²²Z. S. Popovic, S. Satpathy, and R. M. Martin, *Phys. Rev. Lett.* **101**, 256801 (2008).

²³P. Delugas, A. Filippetti, V. Fiorentini, D. I. Bilc, D. Fontaine, and P. Ghosez, *Phys. Rev. Lett.* **106**, 166807 (2011).

²⁴Z. Zhong, P. X. Xu, and P. J. Kelly, *Phys. Rev. B* **82**, 165127 (2010).

²⁵R. Pentcheva and W. E. Pickett, *Phys. Rev. Lett.* **102**, 107602 (2009).

- ²⁶W.-j. Son, E. Cho, B. Lee, J. Lee, and S. Han, *Phys. Rev. B* **79**, 245411 (2009).
- ²⁷P. Blaha, K. Schwarz, G. K. H. Madsen, D. Kvasnicka, and J. Luitz, *WIEN2k, An Augmented Plane Wave + Local Orbitals Program for Calculating Crystal Properties* (Karlheinz Schwarz, Techn. Universität Wien, Austria, 2001).
- ²⁸J. P. Perdew, K. Burke, and M. Ernzerhof, *Phys. Rev. Lett.* **77**, 3865 (1996).
- ²⁹A. A. Mostofi, J. R. Yates, Y.-S. Lee, I. Souza, D. Vanderbilt, and N. Marzari, *Comput. Phys. Commun.* **178**, 685 (2008).
- ³⁰J. Kuneš, R. Arita, P. Wissgott, A. Toschi, H. Ikeda, and K. Held, *Comput. Phys. Commun.* **181**, 1888 (2010).
- ³¹Z. Zhong, P. Wissgott, K. Held, and G. Sangiovanni, *Europhys. Lett.* **99**, 37011 (2012).
- ³²George F. Koster, John O. Dimmock, Robert G. Wheeler, and Hermann Statz, *Properties of the Thirty-Two Point Groups* (MIT Press, Cambridge, MA, 1963).
- ³³A. F. Santander-Syro, O. Copie, T. Kondo, F. Fortuna, S. Pailhès, R. Weht, X. G. Qiu, F. Bertran, A. Nicolaou, A. Taleb-Ibrahimi *et al.*, *Nature (London)* **469**, 189 (2011).
- ³⁴W. Meevasana, P. D. C. King, R. H. He, S.-K. Mo, M. Hashimoto, A. Tamai, P. Songsiriritthigul, F. Baumberger, and Z.-X. Shen, *Nature Mater.* **10**, 114 (2011).
- ³⁵If the antisymmetric hopping H_y is included, we obtain the same behavior as for the dashed line of Figs. 2(c)–2(e).
- ³⁶L. Petersen and P. Hedegard, *Surf. Sci.* **459**, 49 (2000).
- ³⁷H. Nakamura, T. Koga, and T. Kimura, *Phys. Rev. Lett.* **108**, 206601 (2012).
- ³⁸E. Flekser, M. Ben Shalom, M. Kim, C. Bell, Y. Hikita, H. Y. Hwang, and Y. Dagan, *Phys. Rev. B* **86**, 121104 (2012).
- ³⁹A. Joshua, J. Ruhman, S. Pecker, E. Altman, and S. Ilani, *arXiv:1207.7220*.
- ⁴⁰S. Thiel, G. Hammerl, A. Schmehl, C. W. Schneider, and J. Mannhart, *Science* **313**, 1942 (2006).
- ⁴¹A. D. Caviglia, S. Gariglio, N. Reyren, D. Jaccard, T. Schneider, M. Gabay, S. Thiel, G. Hammerl, J. Mannhart, and J.-M. Triscone, *Nature (London)* **456**, 624 (2008).
- ⁴²C. Bell, S. Harashima, Y. Kozuka, M. Kim, B. G. Kim, Y. Hikita, and H. Y. Hwang, *Phys. Rev. Lett.* **103**, 226802 (2009).
- ⁴³M. Ben Shalom, A. Ron, A. Palevski, and Y. Dagan, *Phys. Rev. Lett.* **105**, 206401 (2010).
- ⁴⁴A. D. Caviglia, S. Gariglio, C. Cancellieri, B. Sacépé, A. Fête, N. Reyren, M. Gabay, A. F. Morpurgo, and J.-M. Triscone, *Phys. Rev. Lett.* **105**, 236802 (2010).
- ⁴⁵O. Copie, V. Garcia, C. Bödefeld, C. Carrétéro, M. Bibes, G. Herranz, E. Jacquet, J.-L. Maurice, B. Vinter, S. Fusil *et al.*, *Phys. Rev. Lett.* **102**, 216804 (2009).
- ⁴⁶A. Joshua, S. Pecker, J. Ruhman, E. Altman, and S. Ilani, *Nat. Commun.* **3**, 1129 (2012).
- ⁴⁷G. Khalsa, B. Lee, and A. MacDonald, *arXiv:1301.2784*.